2014

# Experimental Comparison of the Refrigerant Reservoir Position in a Primary Loop Refrigerant Cycle with Optimal Operation

Jan Christoph Menken
*AUDI AG, Germany*, jan-christoph.menken@audi.de

Thomas Weustenfeld
*AUDI AG, Germany*, thomas.weustenfeld@audi.de

Jürgen Köhler
*Technische Universität Braunschweig, Institut für Thermodynamik, Germany*, juergen.koehler@tu-bs.de

# Experimental Comparison of the Refrigerant Reservoir Position in a Primary Loop Refrigerant Cycle with Optimal Operation

Jan Christoph MENKEN[1*], Thomas A. WEUSTENFELD[1*], Juergen KOEHLER[2]

[1] AUDI AG,
Ingolstadt, Germany
Contact Information (jan-christoph.menken@audi.de,
thomas.weustenfeld@audi.de)

[2] TU Braunschweig, Institute of Thermodynamics
Braunschweig, Germany
Contact Information (juergen.koehler@tu-bs.de)

* Corresponding Author

## ABSTRACT

Recent attempts to find energy-efficient thermal management systems for electric and plug-in hybrid electric vehicles have led to secondary loop systems as an alternative approach to meet dynamic heating and cooling demands and reduce refrigerant charge. As such, a thorough understanding of the vapor compression cycle, which serves as the central thermal supply unit, is required. In addition to design considerations concerning the type and size of components such as the heat exchangers or compressor, the refrigerant reservoir choice between a high pressure receiver or a low pressure accumulator is critical for energy-efficient operation under varying operation conditions. In this work, two possible positions of the accumulator/receiver are experimentally examined and optimal control is applied. Therefore, either the superheating at the compressor inlet or outlet of the receiver system or the subcooling at the condenser outlet of the accumulator system are chosen as control variables and adjusted by an electrical expansion valve. Experimental results based on a simple automotive R134a primary loop system containing a scroll compressor are presented. Comparing these two different systems with a receiver or an accumulator, a receiver system shows a slightly higher COP under the examined operation conditions when operated optimally. However the receiver/accumulator position has a non-negligible impact on high and low pressure itself resulting in an advantage for the accumulator system in a cold winter scenario.

## 1. INTRODUCTION

As secondary loop systems become a viable alternative approach for automotive thermal management systems, fundamental design requirements concerning the primary vapor compression cycle need to be specified. The concept of a secondary loop refrigeration system can be found in various fields of application. Wang et al. (2010) offer an extensive review on secondary loop refrigeration systems including performance and risk assessment of flammable refrigerants. Recently, much research has been performed regarding automotive applications in this field. Ghodbane et al. (2007) present a secondary loop system with the HFC refrigerant R152a. Kowsky et al. (2012) demonstrate a hermetic encapsulated central thermal management unit for the use in electric and hybrid vehicles using the battery waste heat as energy source during heat pump mode. The occurring energy storage effects in such systems can even be increased by the addition of phase change materials in the secondary loops (Lemke et al., 2012). This work focuses on the examination and design of a simple automotive primary refrigerant loop containing a compressor, a condenser, an expansion valve, an evaporator and a refrigerant "reservoir". The goal of this work is to provide guidance whether an automotive primary loop refrigerant cycle for secondary loop applications should be equipped with a high pressure reservoir (so-called receiver) or low pressure reservoir (so-called accumulator), however, the procedure can be transferred to non-automotive applications as well.

Jensen and Skogestad (2007) identify the five steady state degrees of freedom (DOF) from a control, operational and design point of view for a simple vapor compression cycle as follows:

(a) compressor power and design

(b) effective heat transfer in condenser (including UA-values)

(c) heat transfer in evaporator (including UA-values)

(d) active refrigerant charge in cycle

(e) choke valve opening

Referring to this list, the compressor power (a) results from a given cooling or heating duty and both condensation (b) and evaporation (c) are limited by their heat exchanger design, therefore only the active refrigerant charge (d) and the valve opening (e) are discussed as the two remaining DOF. However, considering weight- and cost-reduction goals in automotive refrigerant cycles, active charge control is not further discussed in this study due to its additionally required valve. Therefore, the two designs shown in figure 1 will be evaluated in the following, distinguished only by the position of the refrigerant reservoir, which is used for regulating the amount of refrigerant inside the cycle under varying operation conditions. The high pressure receiver is positioned at the condenser outlet and, assuming ideal components,

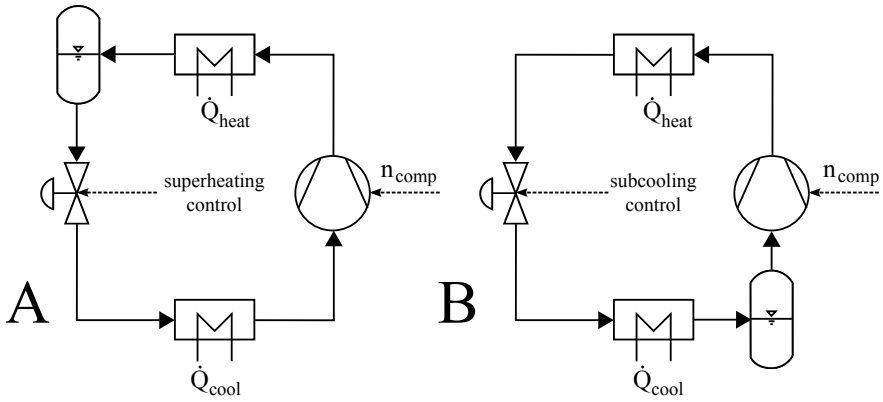


**Figure 1:** Evaluated system designs with either receiver (A) or accumulator (B).

passes saturated liquid refrigerant to the expansion valve. In contrast, an ideal low pressure accumulator is positioned at the evaporator outlet avoiding superheating and transferring only saturated vaporous refrigerant to the compressor. At steady state conditions, both receiver and accumulator should contain a vapor-liquid equilibrium.

## 2. METHODS

### 2.1 Controlled Variables

A schematic of the control system is shown in figure 2. Assuming given flow rates of secondary fluids at the heat exchangers, the compressor speed is used to fulfill load requirements while the electronic expansion valve (EEV) is used either to control the superheat temperature at compressor inlet or outlet in the receiver system or subcooling temperature at the condenser outlet in the accumulator system (equations 1-3).

$$\Delta T_{sup} = T_1 - T_{sat,vap}(p_1) \tag{1}$$

$$\Delta T_{dsh} = T_2 - T_{sat,vap}(p_2) \tag{2}$$

$$\Delta T_{sub} = T_{sat,liq}(p_3) - T_3 \tag{3}$$

Generally, several variables could be used as a controlled variable for system optimization. However, superheating as well as subcooling have been proven in practice and can be directly applied. Additionally, subcooling ensures the exploitation of the entire condensation enthalpy (Jensen and Skogestad, 2007). As the vapor compression cycle is used as both a refrigeration and heat pump device, depending on the load case either the cooling power $\dot{Q}_{cool}$ or heating power $\dot{Q}_{heat}$ is controlled by a PI controller by adapting the compressor speed $n$ accordingly. Cooling and heating power

on the coolant side (see figure 2, left) are calculated using measured coolant mass flow rates ($\dot{m}$) and temperatures at heat exchanger inlet ($T$) and outlet ($T'$)

$$\dot{Q}_{cool} = \dot{m}_e c_{p,e}(T'_e - T_e) \tag{4}$$

$$\dot{Q}_{heat} = \dot{m}_c c_{p,c}(T'_c - T_c). \tag{5}$$

Every refrigeration or heat pump system should be compared at similar loads as the desired system output (either cooling power or heating power) should be provided using minimal energy consumption. Therefore it is necessary to keep $\dot{Q}_{cool}$ or $\dot{Q}_{heat}$ at a defined target value during all experiments. An important indicator for vapor compression cycles is the Coefficient of Performance (COP), defined as follows depending on the load case:

$$COP_{cool} = \dot{Q}_{cool}/P_{comp} \tag{6}$$

$$COP_{heat} = \dot{Q}_{heat}/P_{comp}. \tag{7}$$

Because mass flow measurement is not suitable for mass produced systems, thermal power control (instead of temperature control) is only suitable in a testing environment. The load demand is satisfied by the rotational speed of the compressor. For given inflow temperatures and mass flow rates this means the remaining degree of freedom given by the EEV opening should be used to optimize the operating point by minimizing required compressor power, even under varying operation points during one measuring set.

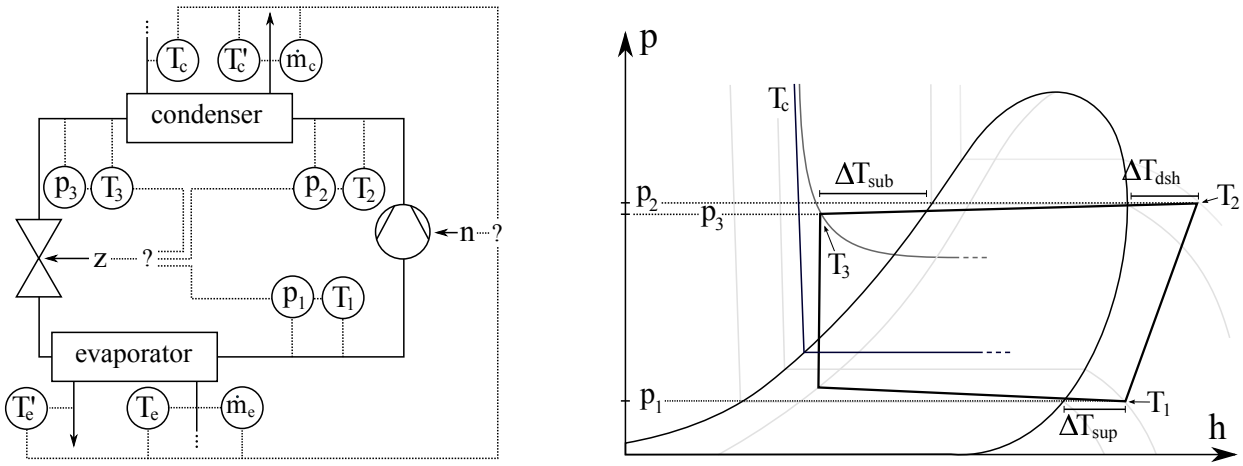


**Figure 2:** Basic control concept: The compressor speed $n$ is used to fulfill load requirements (cooling power or heating power) while the electronic expansion valve is used either to control superheat $\Delta T_{sup}$, discharge superheat $\Delta T_{dsh}$ or subcooling $\Delta T_{sub}$ depending on the system configuration

## 2.2 Test Bed

The test bed used for the experiments consists of a primary R134a refrigeration cycle. To provide constant inlet conditions over a broad range of operation, the coolant side of the test bed is equipped with electric heaters for increasing the temperature as well as cooling units to lower the coolant's temperature. A 50/50 mixture of water and glycerol-based coolant additive is used as coolant in the secondary loops. To minimize installation space and reduce thermal losses, the primary cycle features a compact design. Additionally, all tubes and hoses are insulated. Two automotive plate heat exchangers are used as the evaporator and condenser consisting of 28 and 61 plates respectively. The electronic expansion valve (EEV) with a maximum cross-sectional diameter of 3.5mm varies the cross-sectional area in a range of approximately 1800 steps. The test bed is equipped with a $34cm^3$ commercially available automotive electrical scroll compressor. In contrast to wobble or swash-plate piston compressors, scroll compressors exhibit a higher volumetric efficiency. Because of the operation at higher rotation speed, its displacement volume can be made smaller while achieving the same mass flow rate which leads to a more compact design and lighter weight (Zeng et al., 2001; Gerken and Calhoun, 2000). It should be noted that the compressor's power electronics are flooded with the inlet refrigerant for cooling. This results in a post heat exchanger evaporation caused by the thermal losses of the compressor and means

that the measured pressure and temperature at the compressor inlet do not describe the state of the refrigerant entering the scroll spiral but rather the inlet condition entering the component. Figure 3 details the inner refrigerant flow of the receiver and accumulator. Not only is the compressor inlet state influenced by the internal component cooling, but also by the design of the accumulator. In order to ensure a sufficient oil flow rate in the refrigerant cycle, the J-tube within the accumulator has an oil bleed hole at the bottom. As oil deposition occurs at the bottom of the accumulator, the gaseous refrigerant enters the J-tube and carries away a mixture of oil and liquid refrigerant at the oil bleed hole, therefore the vapor quality of the refrigerant at the accumulator outlet is unsaturated gas (Raiser et al., 2006) as some liquid refrigerant is always transferred towards the compressor. In contrast, the refrigerant at the receiver outlet refrigerant is assumed as saturated liquid. In this test bed, both the receiver's and accumulator's inner volume are approximately $200cm^3$.

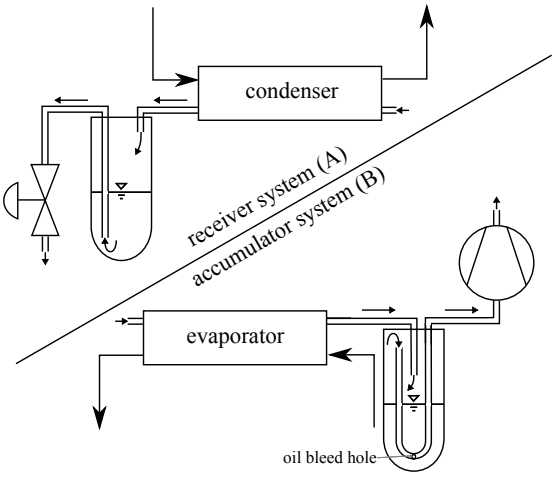


**Figure 3:** Design of receiver and accumulator in refrigerant cycle (excluding dryer elements)

It has to be mentioned, that all experiments are limited by the test bed constraints given in table 1. At certain operation points, this can lead to a restricted performance or non optimal operation. All measurements are sampled every $0.1s$ and smoothed by a moving average filter with window size 100 in order to remove measurement noise. Filtering is also applied before calculating variances.

**Table 1:** Test bed constraints

| | | | | |
|---|---|---|---|---|
| | | $T_2$ | $<$ | $130°C$ |
| | | $p_2$ | $<$ | $28 \times 10^5 Pa$ |
| $0.9 \times 10^5 Pa$ | $<$ | $p_1$ | | |
| $0\%$ | $<$ | $z_{eev}$ | $<$ | $100\%$ |
| $13Hz$ | $<$ | $n_{comp}$ | $<$ | $133Hz$ |

## 2.3 Refrigerant Charge Determination

To guarantee a meaningful comparison of operation efficiency, each system's refrigeration charge must be determined. Generally, the lowest charge possible that is sufficient at high cooling loads is preferred (Poggi et al., 2008). For charge determination in this work, coolant at a temperature of $40°C$ at the condenser and $40°C$ at the evaporator inlet is provided in order to represent high cooling loads. As low refrigerant charge restricts desired heating or cooling loads, the compressor speed is fixed at $75Hz$ for simplification reasons. Initially, each system is charged with $100g$ of refrigerant and successively increased by 30g-40$g$ every 5 minutes. Due to the different system designs, the R134a refrigerant charge is determined as follows:

**Receiver system (A):** The input value for the superheat controller is set to a value of $\Delta T_{sup} = 5K$. As the refrigerant charge is too low, superheating settles at around $55K$ with a maximum EEV cross-sectional area. As more refrigerant is added to the system, the superheat decreases and the EEV begins to operate in its control range. Overfilling results in subcooling and a significant pressure rise.

**Accumulator system (B):** The EEV opening is set to $z_{eev} = 65\%$ which would lead to a subcooling of approximately $5K$ in an appropriately charged cycle. At low refrigerant charge, no subcooling but very large superheating can be detected. The more refrigerant is added to the system, the more the subcooling increases and the superheating decreases. At $\Delta T_{sub} \approx 5K$, the desired subcooling is set to $5K$ by the EEV controller. Overfilling then leads to a maximum EEV cross-sectional area. Therefore, $\Delta T_{sub} = 5K$ can no longer be maintained and increases.

Figure 4 shows the high pressure, $COP_{cool}$ and EEV opening of the receiver and accumulator system. As visualized by a plateau of constant pressure, filling of the refrigerant reservoir marginally affects any refrigerant state of the cycle except the actual filling level within the receiver or accumulator. Assuming an ideal refrigeration charge lying near the center of each plateau, no significant difference in refrigerant charge between the systems can be detected. Therefore, the receiver and accumulator system for this work will be charged with a refrigerant mass of 510$g$. It seems that similar inner volumes of the two different reservoirs result in comparable refrigerant charges. The amount of refrigerant is not further investigated; however it must be noted that the refrigerant charge has significant influence on system performance (Cho et al., 2005) and even the optimal operation point in terms of superheat/subcooling may change depending on the refrigerant charge.

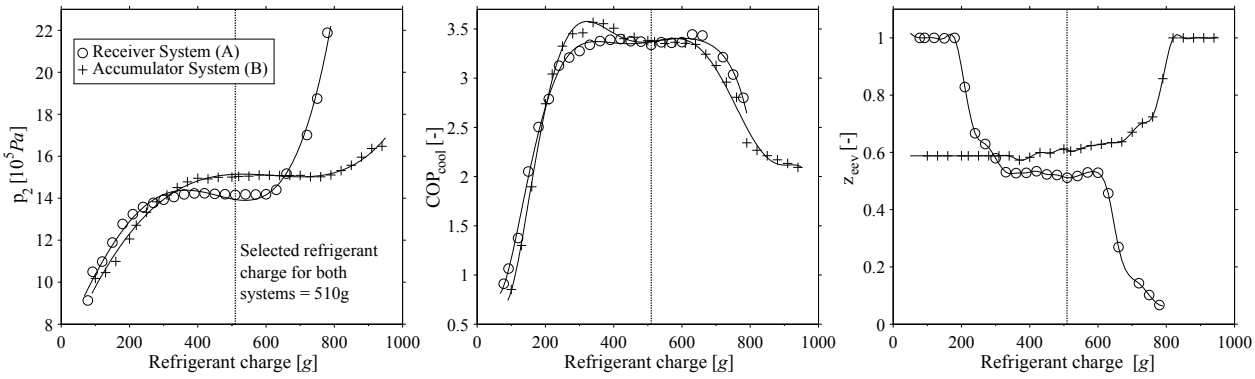


**Figure 4:** Comparison of high pressure $p_2$, $COP_{cool}$ and relative valve opening $z_{eev}$ of both systems for increasing overall refrigeration charge. The chosen charge is marked near the center of the high pressure and $COP_{cool}$ plateau.

## 2.4 Evaluated Use Cases

Due to the fact that an automotive thermal management system is exposed to various environment conditions over the course of a year, different parameters such as temperature, relative humidity and solar radiation must be taken into account. As the coolant-side heat exchanger inlet and outlet can be regarded as the primary cycle's system boundaries, coolant at constant temperature and mass flow rates enters the evaporator and condenser for comparison purpose. Both systems are then evaluated under defined operation conditions assuming steady state operation of a battery electric vehicle in European winter, reheat and summer mode:

**winter mode:** At $T_{amb} = -5°C$, the waste heat of the battery or power electronics is applied as a heat source for the refrigeration cycle which is used as a heat pump. Insufficient waste heat must be compensated by an additional electric heater. As the passenger compartment demands constant heating, the output condensation energy $\dot{Q}_{heat}$ is kept constant.

**reheat mode:** At moderate ambient temperature $T_{amb} = 15°C$ and a relative humidity of $\Phi_{amb} = 50\%$ the moist air entering the passenger compartment is cooled below its dew point leading to condensation. Thereafter, the saturated air is reheated. For simplicity, the vapor compression cycle is assumed to provide a high and low temperature level to realize a reheat. The cooling load $\dot{Q}_{cool}$ is kept constant, resulting in a COP-coupled over-accomplished heating load $\dot{Q}_{heat}$.

**summer mode:** At $T_{amb} = 35°C$ the primary cycle's evaporator provides chilled coolant which fulfills the constant cooling load $\dot{Q}_{cool}$ of the passenger compartment.

**Table 2:** Use cases derived from simple cabin load simulation.

| *Variable* | Winter | Summer | Reheat |
|---|---|---|---|
| $T_e$ $[°C]$ | 10 | 11 | 5 |
| $T_c$ $[°C]$ | 40 | 40 | 27.5 |
| $\dot{Q}_{cool}$ $[W]$ | - | 2000 | 1000 |
| $\dot{Q}_{heat}$ $[W]$ | 3600 | - | - |
| $\dot{m}_e$ $[kg/s]$ | 0.1 | 0.1 | 0.1 |
| $\dot{m}_c$ $[kg/s]$ | 0.1 | 0.1 | 0.1 |

Table 2 summarizes the heat exchanger's inlet conditions derived from simple cabin load simulations of the three use cases. The assumed passenger cabin loads do not include any transient behavior but only the predicted steady state heating or cooling loads. In order to benchmark absolute energy savings, the compressor energy consumption for all three use cases are averaged with weighting factors based on average European weather data and driving behavior for each scenario, calculated to $\omega_{summer} = 0.12$, $\omega_{reheat} = 0.68$ and $\omega_{winter} = 0.2$. These estimates are based on the

temperature distributions of selected European capitals.

## 3. RESULTS

### 3.1 Optimal operation

In this section, the results of optimal operation in terms of optimal subcooling and optimal superheating are presented for both possible system configurations: a vapor compression cycle containing a high pressure receiver (system A) or a low pressure accumulator (system B).

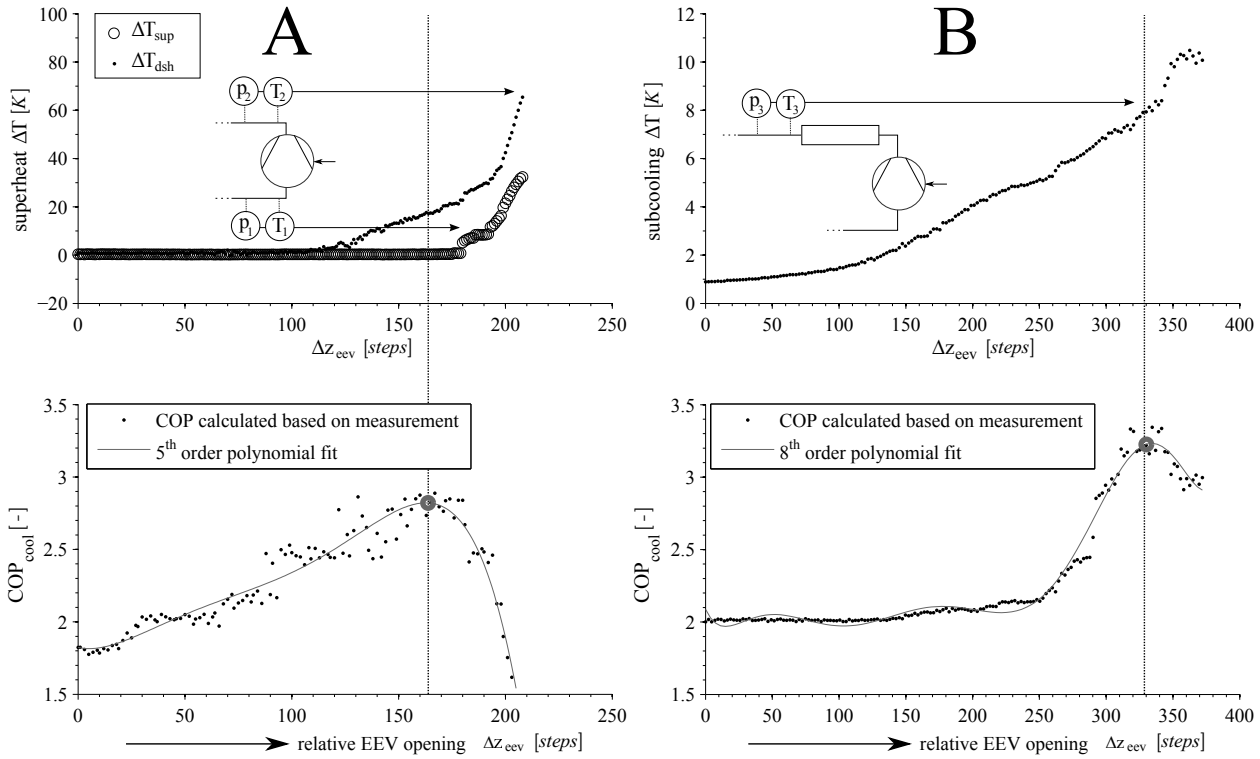


**Figure 5: Left:** Superheating and energy efficiency ($COP_{cool}$) for the receiver system (A). **Right:** Subcooling and energy efficiency ($COP_{cool}$) for the accumulator system (B). The EEV is closed at very slow speed with a $1\%$ change of the opening every 72 minutes (A) / 10 minutes (B) keeping inflow temperatures ($T_e = 5°C$, $T_c = 27°C$), coolant mass flow rates (both $0.1\,\mathrm{kg/s}$) and cooling power ($\dot{Q}_{cool} = 1000W$) constant (reheat case).

In order to verify the existence of an optimal operating point for both system configurations, the expansion valve is closed successively while maintaining constant boundary operating conditions and load: during the experiment, the inlet temperatures and inlet coolant mass flow rates for both heat exchangers are kept constant at $T_e = 5°C$, $T_c = 27°C$ and $\dot{m}_{e/c} = 0.1\,\mathrm{kg/s}$ with a standard deviation of $0.1°C$ for the condenser and $0.4°C$ for the evaporator inlet flow temperature as well as $1.3\,\mathrm{g/s}$ $(1.3\%)$ for both the evaporator and condenser coolant mass flow rate. Cooling power is maintained at $1000W$ with 40W $(4\%)$ standard deviation. In order to eliminate dynamic effects, the expansion valve opening is altered very slowly. This results in a $1\%$ change in cross-sectional area approximately every 72 minutes for the low pressure accumulator system and every 10 minutes for the high pressure receiver system. Different EEV opening speeds are selected to account for different sensitivities of subcooling and superheating.

The results for the reheat use case are exemplarily shown in figure 5. For the receiver system (A), it can be observed that an optimal EEV position exists for the selected operating conditions expressed by a maximum $COP_{cool}$. However, optimal operation is reached before superheating $\Delta T_{sup}$ at evaporator outlet is measured above $0K$. Consequently, the measured state at compressor inlet (component inlet - not spiral inlet) is still unsaturated. Figure 5 also shows that the optimal operating point in terms of discharge superheat $\Delta T_{dsh}$ is situated around $18K$. The results agree e.g. with

Tanawittayakorn et al. (2012), showing that discharge superheat control can result in better performance for certain types of compressors (especially high pressure shell type hermetic compressors). For the accumulator system (B), the optimal operation is achieved when $\Delta T_{sub}$ is close to $8K$. The existence of such optimal subcooling, which is different from $0K$, is discussed generally in Jensen and Skogestad (2007) and experimentally in Pottker and Hrnjak (2012).

**Table 3:** Optimal operation at steady state for system A and B at four defined use cases: cold winter ($i = 1$), winter ($i = 2$), mild winter ($i = 3$), reheat ($i = 4$). Controlled variables are shown in bold text.

| | | *Receiver System (A)* $[k = 1]$ | | | | *Accumulator System (B)* $[k = 2]$ | | | | *Correlations* $c_{j,k}$ | | |
|---|---|---|---|---|---|---|---|---|---|---|---|---|
| $j \downarrow$ | | $i = 1$ | $i = 2$ | $i = 3$ | $i = 4$ | $i = 1$ | $i = 2$ | $i = 3$ | $i = 4$ | $k = 1$ | $k = 2$ | $\lvert c_{j,k}\rvert$ |
| $T_e$ $[°C]$ | $x_1$ | **25.16** | **10.38** | **14.99** | **5.00** | **25.12** | **10.41** | **15.00** | **5.00** | -32% | 8% | |
| $T_c$ $[°C]$ | $x_2$ | **52.00** | **40.00** | **35.00** | **27.51** | **52.00** | **40.00** | **35.00** | **27.51** | 9% | 44% | |
| $\dot{Q}_{cool}$ $[W]$ | $x_3$ | -2614.11 | -2022.39 | -1437.14 | **-999.78** | -2564.43 | -1947.37 | -1394.52 | **-999.59** | -22% | -55% | |
| $\dot{Q}_{heat}$ $[W]$ | $x_4$ | **4499.59** | **3598.55** | **1900.88** | 1420.43 | **4500.88** | **3600.64** | **1898.44** | 1597.91 | 37% | 65% | |
| $P_{comp}$ $[W]$ | $x_5$ | 1997.02 | 1626.08 | 464.40 | 295.68 | 2051.05 | 1621.01 | 477.30 | 313.20 | 46% | 70% | |
| $n_{comp}$ $[Hz]$ | $x_6$ | 70.76 | 79.17 | 23.91 | 22.45 | 63.41 | 63.51 | 24.10 | 23.21 | 64% | 83% | |
| $z_{eev}$ $[\%]$ | $x_7$ | 40.35 | 24.05 | 10.35 | 4.50 | 21.26 | 5.63 | 4.41 | 5.30 | 25% | 6% | |
| $p_1$ $[10^5 Pa]$ | $x_8$ | 2.74 | 1.72 | 3.22 | 2.36 | 3.14 | 2.00 | 3.13 | 2.38 | -97% | -57% | |
| $p_2$ $[10^5 Pa]$ | $x_9$ | 18.48 | 12.98 | 10.26 | 7.97 | 20.35 | 17.88 | 10.99 | 8.82 | 15% | 71% | |
| $\Delta T_{e-c}$ $[K]$ | $x_{10}$ | 26.83 | 29.62 | 20.01 | 22.51 | 26.88 | 29.59 | 20.00 | 22.51 | 84% | 90% | |
| $\Pi$ $[-]$ | $x_{11}$ | 6.74 | 7.56 | 3.19 | 3.37 | 6.48 | 8.95 | 3.51 | 3.71 | 69% | 98% | |
| $\Delta T_{sup}^{opt}$ $[K]$ | $x_{12}$ | 1.51 | 1.65 | 1.04 | 1.36 | 1.44 | 1.54 | 1.04 | 1.17 | 93% | 87% | |
| $k \downarrow$ | | | | | | | | | | | | 0.0 0.25 0.5 0.75 1.0 |
| $\Delta T_{dsh}^{opt}$ $[K]$ | $y_1$ | 16.41 | 26.50 | 5.23 | 19.14 | 1.87 | 15.86 | 1.96 | 16.58 | 100% | - | System A |
| $\Delta T_{sub}^{opt}$ $[K]$ | $y_2$ | 0.32 | 0.81 | 0.59 | 0.61 | 12.81 | 22.55 | 8.20 | 7.82 | - | 100% | System B |

More experiments for both systems are carried out using the same procedure in order to examine the displacement of the optimum. As winter and summer case result in similar operating points with comparable heat flows at the heat exchangers and thus do not provide additional information on the shifting of optimal superheating or subcooling, two more winter cases ($i = 1$, $i = 3$) are evaluated. The results are summarized in table 3. Additionally, correlations $c$ between various system variables ($x_j$) and optimal operation point ($y_k$), given by $\Delta T_{dsh}^{opt}$ or $\Delta T_{sub}^{opt}$ are obtained from

$$c_{j,k} = \frac{1}{n-1} \sum_{i=1}^{n} \frac{(x_{i,j} - \mu_j)(y_{i,j} - \mu_j)}{\sigma_{x,j} \cdot \sigma_{y,k}} \tag{8}$$

For the accumulator system (B), correlations are found between optimal subcooling $\Delta T_{sub}^{opt}$ and compressor speed $n_{comp}$ (83%), inlet temperature difference $\Delta T_{e-c}$ (90%) and pressure ratio $\Pi$ (98%). A linear correlation between pressure ratio $\Pi$ and optimal discharge superheating $\Delta T_{dsh}^{opt}$ is described by Tanawittayakorn et al. (2012) for hermetic shell type compressors. In table 3 it can be seen that these quantaties correlate (69%) for the presented system, however an even stronger correlation between $\Delta T_{dsh}^{opt}$ and inlet temperature difference $\Delta T_{e-c} = T_c - T_e$ can be seen (84%). The highest absolute correlation is found between $\Delta T_{dsh}^{opt}$ and low pressure $p_1$ (-97%). The optimal subcooling for the accumulator system (B) varies from $6.9K$ to $22.6K$ depending on the boundary conditions and shows that the optimum can differ from a subcooling of $4 - 5K$ as commonly applied in refrigeration applications. This points out that optimal subcooling or superheating can be predicted from measured system variables. However, a systematic analysis is necessary.

### 3.2 Steady state system comparison

After determining the optimal operation conditions in terms of (discharge) superheating $\Delta T_{sup}/\Delta T_{dsh}$ and subcooling $\Delta T_{sub}$, both system configurations are compared at steady state based on the three defined use cases of section 2.4. Additionally, results for non-optimal operation are provided as well. This allows to relate system design to system operation. For the receiver system (A), $\Delta T_{sup}$ is set $1K$ to guarantee fully evaporated refrigerant at compressor inlet (even higher superheating is common). For the accumulator system (B), $\Delta T_{sub} = 4.5K$ is chosen. The efficiencies for both system designs with either optimal ($\Delta T_{dsh} = \Delta T_{dsh}^{opt}$ or $\Delta T_{sub} = \Delta T_{sub}^{opt}$) or conservative non-optimal ($\Delta T_{sup} = 1K$ or $\Delta T_{sub} = 4.5K$) steady state control are shown in figure 6 for all three use cases as well as absolute combined energy savings $P_{comb}$ based on the weighting factors $\omega$ defined in section 2.4. For all cases, the high pressure receiver

system (A) at $\Delta T_{sup} = \Delta T_{sup}^{opt}$ shows improved energy efficiency over the low pressure accumulator system (B) configuration at $\Delta T_{sub} = \Delta T_{sub}^{opt}$. This results in an overall combined compressor power saving of 8% for the receiver system (A).

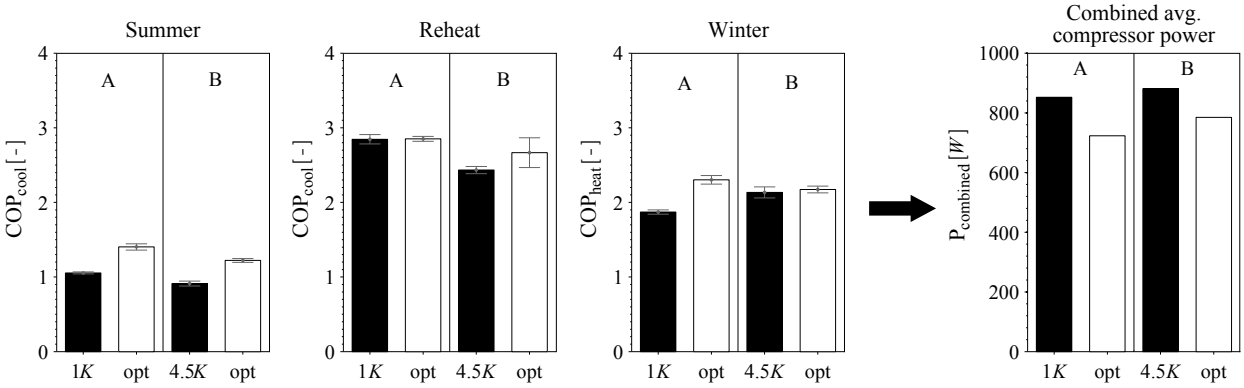


**Figure 6:** Comparison of a simple primary loop refrigerant cycle containing a receiver or accumulator for different load cases at steady state.

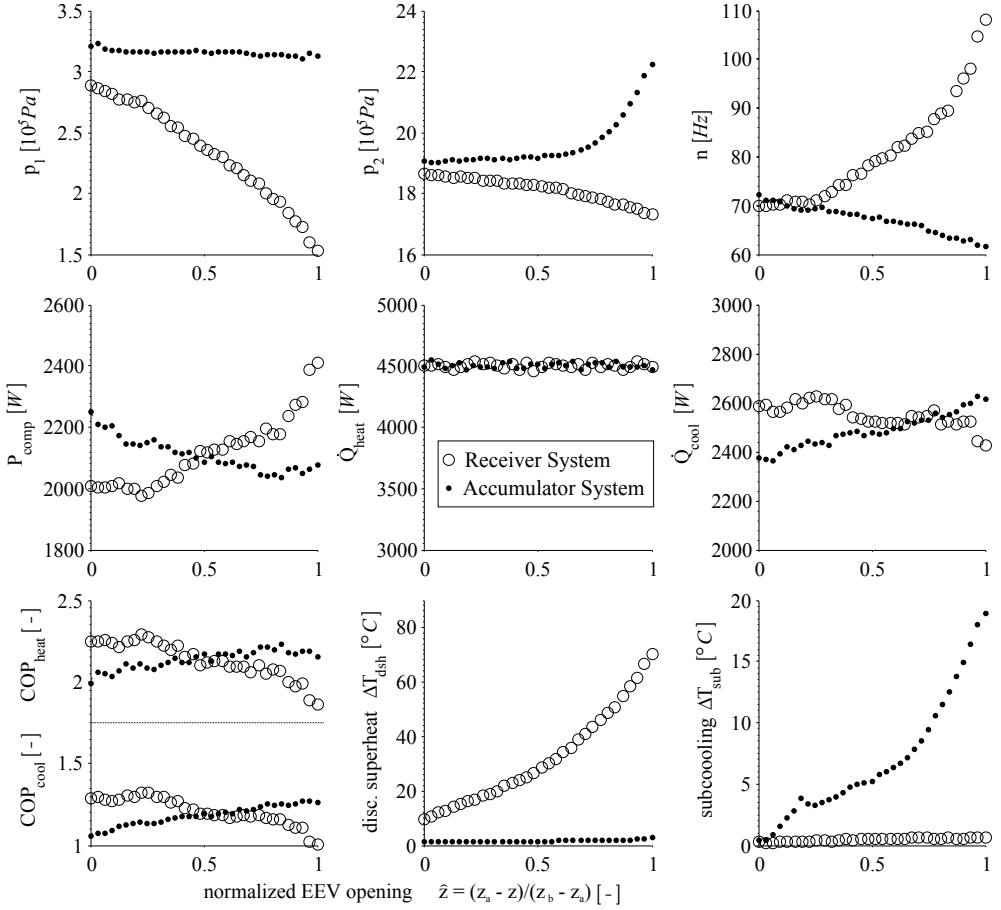


**Figure 7:** System with high pressure receiver compared to a system with low pressure accumulator at the same operating point: Inflow temperatures ($T_e = 25°C \pm 0.3°C$, $T_c = 52°C \pm 0.5°C$), mass flow rates (both $0.1\,^{kg}/_{s} \pm 0.002\,^{kg}/_{s}$) and heat load ($\dot{Q}_{heat} = 4500W \pm 99W$) are kept constant.

Apart from efficiency evaluation, a refrigeration system is limited by several constraints potentially preventing optimal operation, which should be taken into account for a comprehensive comparison. While operating at moderate loads, operational constraints can have a high impact on the efficiency when heating or cooling load are further increased. Additionally, the more heat exchanger inlet temperatures spread apart, the more these constraints become relevant. Two cases are likely to occur: (a) maximum high pressure $p_2$ is reached due to high load $\dot{Q}_{cool/heat}$ and high inlet flow temperatures $T_c$ at the condenser or (b) minimum low pressure $p_1$ is reached due to high load $\dot{Q}_{cool/heat}$ and low inlet flow temperatures $T_e$ at the evaporator. In such a case, an efficient control strategy has to abandon optimal operation and instead influence high or low pressure so that the constraints ($p_1 \geq p_{min}$ and $p_2 \leq p_{max}$, listed in table 1) are not violated while satisfying load requirements. Assuming a compressor controller which is regulating heating/cooling demands, the constraints can only be satisfied by adapting the EEV opening. The influence of the (normalized) EEV opening at constant operation conditions and cooling loads is shown in figure 7. The normalized EEV opening $\hat{z}$ is given by $\hat{z} = (z_a - z)/(z_b - z_a)$ where $z_a$ is the maximum stable EEV opening, $z_b$ is the minimum EEV opening that can be realised without violating any constraints and $z$ is the actual opening value. Clearly, the receiver/accumulator position has a non-negligible impact on high and low pressure. For the low pressure accumulator system (B), closing the EEV will result primarily in an increasing pressure on the high pressure side. Similarly, closing the EEV of the high pressure receiver system (A) primarily results in decreasing pressure on the low pressure side. This implies an advantage for the accumulator system (B) during heat pump mode with a low temperature source, because a higher pressure on the low pressure side at constant loads permits a lower coolant inlet temperature at the evaporator without violating low pressure constraints of the vapor compression cycle. For the heat pump mode with high temperature sink, system (A) should be favored, because high pressure is the limiting variable when condenser inlet temperature increases. In summary, system (B) might be superior when heating at cold temperatures, system (A) might be superior at high temperatures and when sufficient heat at the evaporator side is available. Air conditioning mode is less affected as system operation always stays between roughly $-5°C$ (required by HVAC) and $55°C$ (limited by ambient heat exchanger) assuming ambient temperatures below $45°C$.

## 4. CONCLUSION

Two very similar R134a vapor compression cycles for an automotive secondary loop system were compared applying different steady state operation schemes. The essential difference between these cycles is the placement of the refrigerant "reservoir", which is either a high pressure receiver (A) at the condenser outlet or a low pressure accumulator (B) at the compressor inlet. An internal heat exchanger or a subcooling heat exchanger were intentionally not considered in order to compare two simple systems that are as similar as possible in cost, weight and complexity. For the setup in this work, no significant difference in optimal refrigerant charge was found. Comparing a system with a receiver (A) or an accumulator (B), it is necessary to compare both systems at their respective optimal operating points. Discharge superheating $\Delta T_{dsh}$ for system (A) and subcooling $\Delta T_{sub}$ for system (B) are suited variables to measure optimal operation. By experimentally changing the electronic expansion valve's cross-sectional area at very slow rates, optimal values for $\Delta T_{dsh}$ and $\Delta T_{sub}$ were estimated, allowing comparison of both systems at their optimal operating points as well as at typical operating points common for refrigeration applications ($\Delta T_{sup}$ close to $1K$, $\Delta T_{sub} = 4 - 5K$).

As shown in the results, a receiver system (A) shows superior overall performance compared to the accumulator system (B) under the examined use cases if the receiver system (A) is operated at the optimal discharge superheating temperature $\Delta T_{dsh}^{opt}$. As the implemented scroll type compressors allow suction refrigerant at a slightly unsaturated state, this is a feasible approach. However, the receiver/accumulator position has a non-negligible impact on high and low pressure making the accumulator system in a cold winter heat pump scenario preferable. Besides the impact on the refrigerant reservoir position, it has been shown that steady state operation regarding superheating or subcooling control both have a significant influence on the system's COP. Further work has to be done in order to predict these optimal operation points depending on the inlet conditions and system loads for improving the overall system's performance.

## NOMENCLATURE

### Symbols

| | | |
|---|---|---|
| $c$ | correlation | $(-)$ |
| $c_p$ | specific heat capacity | $(^{kJ}/_{kg})$ |
| $\dot{m}$ | mass flow rate | $(^{kg}/_{s})$ |
| $n$ | rotational speed | $(Hz)$ |
| $p$ | pressure | $(Pa)$ |
| $P$ | electrical power | $(W)$ |
| $\dot{Q}$ | heat flow | $(W)$ |
| $T$ | temperature | $(°C)$ |
| $z$ | valve opening | $(-)$ |
| $\mu$ | mean value | $(-)$ |
| $\Pi$ | pressure ratio | $(-)$ |
| $\sigma$ | standard deviation | $(-)$ |
| $\Phi$ | relative humidity | $(\%)$ |
| $\omega$ | weighting factor | $(-)$ |

### Subscripts

| | |
|---|---|
| amb | ambient |
| c | condenser |
| comp | compressor |
| cool | cooling load |
| dsh | discharge superheat (at compressor outlet) |
| eev | electronic expansion valve |
| e | evaporator |
| heat | heating load |
| liq | liquid |
| opt | optimal |
| sat | saturated |
| sub | subcooling (at condenser outlet) |
| sup | superheat (at evaporator outlet) |
| vap | vapor |

### Acronyms

| | |
|---|---|
| COP | coefficient of performance |
| DOF | degree of freedom |
| EEV | electronic expansion valve |

## REFERENCES


Cho, H., Ryu, C., Kim, Y., and Kim, H. Y. (2005). Effects of refrigerant charge amount on the performance of a transcritical $CO_2$ heat pump. *International Journal of Refrigeration*, 28:1266--1273.

Gerken, D. T. and Calhoun, J. (2000). Design review of cast aluminum scroll compressor components. *SAE Technical Paper*, 2000-03-06.

Ghodbane, M., Craig, T. D., and Baker, J. A. (2007). Demonstration of an energy-efficient secondary loop HFC-152a moile air conditioning system. Final Report for the U.S. Environmental Protection Agency.

Jensen, J. B. and Skogestad, S. (2007). Optimal operation of simple refrigeration cycles part I: Degrees of freedom and optimality of sub-cooling. *Journal Of Computers and Chemical Engineering*, 31:712--721.

Kowsky, C., Wolfe, E., Leitzel, L., and Oddi, F. (2012). Unitary HPAC system. *SAE International Journal of Passenger Cars - Mechanical Systems*, 5(2).

Lemke, N. C., Lemke, J., and Koehler, J. (2012). Secondary loop systems for automotive HVAC units under different climatic conditions. In *International Refrigeration and Air Conditioning Conference at Purdue*, pages 1--10.

Poggi, F., Macchi-Tejeda, H., Leducq, D., and Bontemps, A. (2008). Refrigerant charge in refrigeration systems and strategies of charge reduction. *International Journal of Refrigeration*, 31:353--370.

Pottker, G. and Hrnjak, P. S. (2012). Effect of condenser subcooling of the performance of vapor compression systems: Experimental and numerical investigation. In *International Refrigeration and Air Conditioning Conference at Purdue*, page 1328.

Raiser, H., Heckenberger, T., Tegethoff, W., Koehler, J., and Foersterling, S. (2006). Transient behaviour of R744 vehicle refrigeration cycles and the influence of the suction side accumulator design. *SAE Technical Paper*, 2006-01-0162.

Tanawittayakorn, W., Phrajunpanich, P., and Siwapornphaisarn, S. (2012). Heat pump efficiency improvement by discharge superheated control. In *International Refrigeration and Air Conditioning Conference at Purdue*, page 1197.

Wang, K., Eisele, M., Hwang, Y., and Radermacher, R. (2010). Review of secondary loop refrigeration systems. *International Journal of Refrigeration*, 33(2).

Zeng, X., Major, G. A., Hirao, T., Sekita, M., and Fujitani, M. (2001). Automotive A/C system integrated with electrically-controlled variable capacity scroll compressor and fuzzy logic refrigerant flow management. *SAE Technical Paper*, 2001-01-0587.